MOLECULAR AND CELLULAR BIOLOGY, Feb. 2002, p. 866–873 Vol. 22, No. 3
0270-7306/02/$04.00+0 DOI: 10.1128/MCB.22.3.866–873.2002

Molecular Motor KIF1C Is Not Essential for Mouse Survival and Motor-Dependent Retrograde Golgi Apparatus-to-Endoplasmic Reticulum Transport

Kazuo Nakajima, Yosuke Takei, Yosuke Tanaka, Terunaga Nakagawa, Takao Nakata, Yasuko Noda, Mitsutoshi Setou, and Nobutaka Hirokawa*

Department of Cell Biology and Anatomy, Graduate School of Medicine, University of Tokyo, Bunkyo-ku, Tokyo 113-0033, Japan

Received 16 July 2001/Returned for modification 28 August 2001/Accepted 30 October 2001

KIF1C is a new member of the kinesin superfamily of proteins (KIFs), which act as microtubule-based molecular motors involved in intracellular transport. We cloned full-length mouse *kif1C* cDNA, which turned out to have a high homology to a mitochondrial motor KIF1Bα and to be expressed ubiquitously. To investigate the in vivo significance of KIF1C, we generated *kif1C*$^{-/-}$ mice by knocking in the β-galactosidase gene into the motor domain of *kif1C* gene. On staining of LacZ, we detected its expression in the heart, liver, hippocampus, and cerebellum. Unexpectedly, *kif1C*$^{-/-}$ mice were viable and showed no obvious abnormalities. Because immunocytochemistry showed partial colocalization of KIF1C with the Golgi marker protein, we compared the organelle distribution in primary lung fibroblasts from *kif1C*$^{+/+}$ and *kif1C*$^{-/-}$ mice. We found that there was no significant difference in the distribution of the Golgi apparatus or in the transport from the Golgi apparatus to the endoplasmic reticulum (ER) facilitated by brefeldin A between the two cells. This retrograde membrane transport was further confirmed to be normal by time-lapse analysis. Consequently, KIF1C is dispensable for the motor-dependent retrograde transport from the Golgi apparatus to the ER.

Cells employ microtubule motors for intracellular organelle transport. Kinesin superfamily proteins (KIFs) have been identified as the major molecular motors of microtubule-based intracellular transport (2, 10, 21). There are a total of 45 KIFs in mice (19). Each member of the KIFs consists of a globular head domain and a tail domain. The motor head domain, which is conserved among KIFs, binds to microtubules and hydrolyzes ATP to obtain the energy needed to move toward either the plus or minus end of the microtubules. In contrast, the tail domains are greatly divergent among KIFs and are involved in specific association with their cargoes via adapter proteins (20, 31, 32). Among these KIFs, we have characterized KIF1 subfamily (KIF1A, KIF1Bα, KIF1Bβ, and KIF1C) by sequence similarity and an AF-6/cno domain just C-terminally adjacent to the motor head. Our previous study revealed an individual function of each motor. KIF1A is a plus-end-directed monomeric neuron-specific motor protein and is used for anterograde translocation of synaptic vesicle precursors (27, 40). KIF1B has at least two splice variants: KIF1Bα transports mitochondria (25), and KIF1Bβ transports synaptic vesicle precursors as efficiently as does KIF1A (41). Here, KIF1C is the latest identified protein in this subfamily and is expressed in a wide variety of tissues (21). Human KIF1C has been described to interact with the ezrin domain of protein-tyrosine phosphatase PTPD1, and the overexpression of its dominant negative form perturbed the Golgi-to-endoplasmic-reticulum (ER) retrograde transport (5). On treatment with brefeldin A (BFA), the Golgi apparatus quickly forms membrane tubules (18), which move along microtubules and fuse with the ER, resulting in a dramatic breakdown of the Golgi apparatus, whose components redistribute into the ER by suppression of the ER-to-Golgi membrane transport (17). In this way, the Golgi-to-ER transport can be enhanced for observation (15).

To determine the significance of KIF1C in vivo, we cloned the mouse *kif1C* gene and disrupted it by gene targeting. This is the latest study in the series of KIF mouse knockouts (14, 26, 33, 34, 40, 41). Contrary to our expectations, mice deficient in KIF1C exhibited no apparent abnormalities. Also, we show at the subcellular level that microtubule-dependent Golgi-to-ER retrograde transport works normally even in the absence of the KIF1C motor, which suggests functional redundancy in other microtubule motors in vivo.

MATERIALS AND METHODS

cDNA cloning of mouse *kif1C* gene. A partial sequence of *kif1C* was identified by a previous reverse transcription-PCR (RT-PCR) search of new motors by using degenerate primers corresponding to the kinesin motor consensus sequences from mouse brain cDNA (21). Using this fragment as a probe, the 5′ half (3 kb) of the cDNA was isolated from a λ phage library of mouse brain cDNA. The remaining carboxyl-terminal region was obtained by RT-PCR cloning from mouse spinal cord cDNA based on the human sequence (5). The amplified fragments were subcloned into pBluescriptII SK(+), and more than 10 clones were sequenced to confirm its integrity.

Subcellular fractionation. MDCK cells were grown in 10-cm plastic transplate dishes (Corning). The cells were lysed with cold phosphate-buffered saline containing protease inhibitors. The lysate was successively centrifuged at 10,000 × *g* and 20,000 × *g* using a benchtop centrifuge (Tomy) and at 30,000 × *g* and 100,000 × *g* using an ultracentrifuge (Beckman). Samples from each fraction were analyzed by immunoblotting.

Microtubule binding assay of KIF1C. The microtubule motor protein fraction including KIF1C was prepared from mouse brain lysate, and nucleotide-dependent microtubule binding activity was assayed as previously described (35).

* Corresponding author. Mailing address: Department of Cell Biology and Anatomy, Graduate School of Medicine, University of Tokyo, 7-3-1 Hongo, Bunkyo-ku, Tokyo 113-0033, Japan. Phone: 81-3-5841-3326. Fax: 81-3-5802-8646. E-mail: hirokawa@m.u-tokyo.ac.jp.

Gene targeting of the *kif1C* gene. The targeting vector was constructed using genomic clones obtained from a λEMBL3 genomic library of embryonic stem (ES) cell line J1 (34), pMC1-DTA negative selection cassette (39), and pIRESβgeopolyA positive selection cassette for promoter trapping (see Fig. 2). pIRESβgeopolyA was applied in the forward direction and flanked by a 1.3-kb *Bam*HI-*Sma*I 5′ homologous region and an 8.0-kb *Sma*I-*Spe*I 3′ homologous region. Reversed pMC1-DTA without a poly(A) signal was ligated at the 5′ extremity. A splicing acceptor sequence (36) was inserted between the 5′ homologous region and the internal ribosome entry site (IRES) sequence.

The targeting vector was linearized with *Xho*I and electroporated into the ES cell line J1. Homologous recombinant clones were isolated as described previously (13). The homologous recombination events were identified in 7 of 228 clones; therefore the targeting efficiency was 3%. The recombinants were injected into blastocysts as described previously (8). Chimeric male mice were bred with C57BL/6J females, and agouti offsprings were generated from two independent clones, indicating germ line transmission of the ES genome.

Genotyping of animals. Mouse tail samples were processed and subjected to PCR amplification for the *neo* transgene (34) and an intronic sequence from the deleted region. The latter was detected as a 227-bp band with 5′-TGCACTCC CTACCCCTAAGGTG-3′ and 5′-GACAGGAGAGTGAAGGTGCTTGG-3′. Southern blotting was also performed using a standard method (13).

Histological analysis. Mice were anesthetized and fixed by perfusion with FEA solution (5% formalin, 70% ethanol, 5% acetic acid). The fixed samples were then washed, dehydrated, cleared, and embedded in Paraplast (Oxford Labware). The blocks were cut using a rotatory microtome (HM-355; Carl Zeiss) into 10-μm-thick serial sections. They were mounted onto glass slides, deparaffinized, and stained with hematoxylin-eosin (for heart, kidney, and lung tissues) or silver-gold (for brain tissue) by the method of Bodian (4).

For LacZ staining of the tissues, mice were anesthetized with ether and perfused with 0.2% glutaraldehyde in 0.1 M phosphate buffer (pH 7.3) supplemented with 5 mM EGTA and 2 mM $MgCl_2$. The tissues were then sliced with a Vibratome (D.S.K.MicroSlicer) and postfixed for 1 h. The postfixed samples were processed as described previously (11), embedded in Paraplast, and cut into 10-μm-thick serial sections as described above.

Immunoblotting and immunochemistry. Anti-KIF1C polyclonal antibodies were raised in rabbits against a C-terminal synthetic peptide of KIF1C (see Fig. 1A). The serum was affinity purified with the antigen using a SulfoLink column (Pierce). Immunoblotting was performed using mouse tissue homogenates as described previously (8).

For immunohistochemistry, fresh livers from either $kif1C^{+/+}$ or $kif1C^{-/-}$ mice were frozen with liquid 2-methylbutane. Samples were sectioned with a cryostat into 14-μm-thick sections, fixed with cold methanol, and dried. Subsequently, the sections were further fixed with 2% paraformaldehyde in phosphate-buffered saline for 15 min, blocked with 10% normal goat serum for 30 min and then incubated with an anti-KIF1C polyclonal antibody at 4°C overnight.

Mouse lung fibroblasts were primary cultured from the $kif1C^{+/+}$ and $kif1C^{-/-}$ mice by the standard method (7, 9). The cells were grown at 37°C in 5% CO_2 on coverslips in Dulbecco's modified Eagle's medium (Gibco BRL) supplemented with 10% fetal calf serum (JRH Biosciences) and penicillin-streptomycin. The cells were fixed and permeabilized with 2% paraformaldehyde for 10 min followed by 0.1% Triton X-100 for 10 min; alternatively, cold methanol was used for 5 min at −20°C. The blocking reagent was 10% normal goat serum. Red-fluorescent Alexa Fluor 568-labeled goat anti-mouse immunoglobulin G and green-fluorescent Alexa Fluor 488-labeled goat anti-rabbit immunoglobulin G, anti-p58 antibody, and anti-GM-130 and anti-Vti1b antibodies were purchased from Molecular Probes, Sigma, and Transduction Laboratories, respectively. Observation was carried out with a Zeiss LSM510 confocal laser-scanning microscope.

Golgi tubule formation assay. To visualize the dynamics of the Golgi structure in living cells, the cells were transfected with a pEYFP (enhanced yellow fluorescent protein)-human β1,4-galactosyltransferase fusion protein gene construct (Clontech) by the calcium phosphate method for 6 to 12 h using a Cell Phect kit (Pharmacia), washed three times in Hanks' balanced salt solution (Gibco BRL), and then incubated in complete medium for several hours before observation. After the addition of BFA (Epicentre Technologies) at 10 μg/ml at 30°C, time-lapse images were obtained using a confocal laser-scanning microscope (Bio-rad MRC-1024) on an Axiovert100 equipped with a Kr/Ar laser (Zeiss) and a 40× water-immersion lens (Zeiss) (24). Images were processed using NIH image software (Wayne Rasband, Research Service Branch, National Institutes of Health, Bethesda, Md.) and Adobe Photoshop software (Adobe, San Jose, Calif.).

Nucleotide sequence accession number. The DDBJ-GenBank accession number of the murine *kif1C* gene is AB074017.

RESULTS

Cloning of the murine *kif1C* gene. We identified the mouse *kif1C* gene through our previous systematic RT-PCR search for new KIFs from brain cDNA by using degenerate primers corresponding to kinesin motor consensus sequences (21). Using the *kif1C* PCR fragment as a probe, we cloned the full-length cDNA of the mouse *kif1C* gene, which consists of 1,100 amino acids (aa), with a conserved motor domain at its N terminal. Comparison of the sequence of the mouse KIF1C (mKIF1C) to those of other KIF members, human KIF1C (hKIF1C), mouse KIF1Bα (mKIF1Bα), and mouse KIF1A (mKIF1A), is shown in Fig. 1A. A kinesin motor head domain, which is conserved among all of the KIFs, was found at aa 1 to 355. A KIF1 subfamily consensus domain, which includes AF-6/cno (aa 486 to 602) and the FHA domain (aa 499 to 624), was also found at aa 356 to 670 of KIF1C. These domains have been thought to be involved in protein-protein interactions (28, 38). Interestingly, the tail of mKIF1C is homologous to that of mKIF1Bα but not to that of mKIF1A and mKIF1Bβ, suggesting that two functionally different subclasses exist within the KIF1 subfamily.

We have raised a polyclonal antibody against a C-terminal peptide sequence of KIF1C (Fig. 1A), which was specific to KIF1C and recognized a 150-kDa band in the total homogenate of mouse brain. Immunoblotting showed a ubiquitous expression pattern of KIF1C (Fig. 1B), which confirmed previous data (5, 21). Subcellular fractionation showed that KIF1C was distributed most abundantly in the high-speed pellet fractions, which suggested that KIF1C was associated with membranes of smaller vesicles in cells (Fig. 1C). We then examined the nucleotide dependency of the KIF1C-microtubule interaction. The native KIF1C protein was associated with and dissociated from microtubules in the presence of the nonhydrolyzable ATP analog AMP-PNP and ATP, respectively (Fig. 1D). This result suggested that interaction of KIF1C with microtubules was coupled to ATP hydrolysis, a mechanism similar to that found with conventional kinesin (35).

Targeted disruption of the *kif1C* gene. To investigate the in vivo function of KIF1C, the murine *kif1C* gene was disrupted by gene targeting with a promoter trap strategy. We knocked in a β*geo* (β-galactosidase-*neo*) fusion gene into the *kif1C* locus, which enabled us to assess its expression pattern concurrently (Fig. 2A). The β*geo* fusion gene was inserted just downstream of the ATG-containing exon, which led to translation of a small portion of the KIF1C head region (aa 1 to 35) in addition to the β*geo* fusion protein. The expressed portion of the head region did not contain either the motor consensus or the cargo binding property, so that it may be nonfunctional. After the targeting vector was transfected in ES cells, the recovered genomic DNA from Neo^r colonies was digested with *Pst*I and analyzed for the homologous recombination by Southern blotting. Seven independent homologous recombinant clones were identified, and six of them were microinjected into (C57BL/6J × BDF_1 blastocysts; Two independent mouse strains were established and used in future analyses. Southern blotting of the pups revealed the predicted patterns of gene disruption (Fig. 2B).

Cross-breeding between the heterozygotes generated mice of each genotype following the Mendelian ratio, suggesting

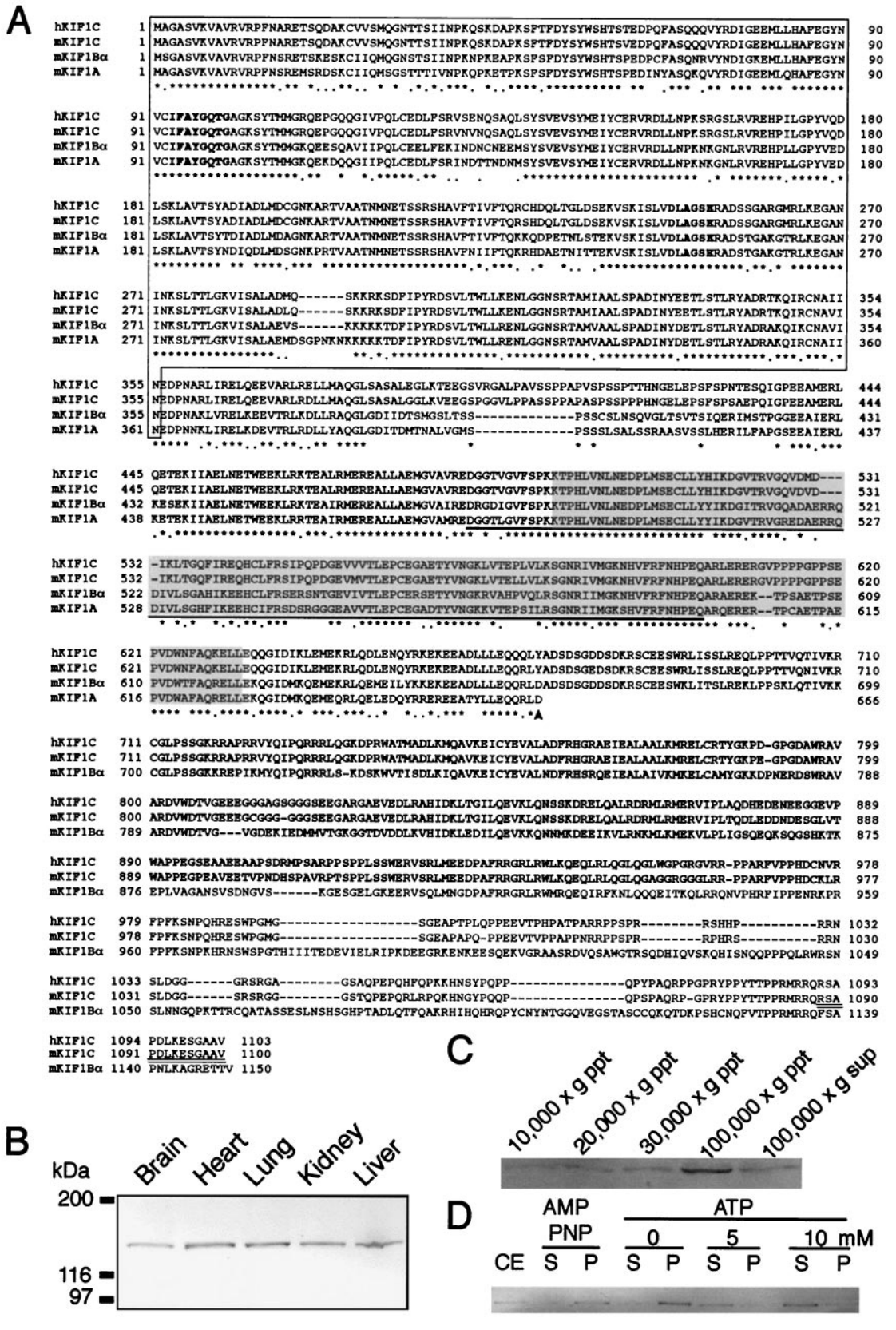

FIG. 1. Molecular cloning of the mouse *kif1C* gene. (A) Amino acid sequence alignment of the mammalian KIF1 subfamily members. Amino acids are numbered on the left and right sides of the sequence. Asterisks indicate identical amino acids, and dots show similar residues among four proteins. The kinesin head domain, which is conserved between conventional kinesin and the KIF1 family, is boxed. Major consensus sequences

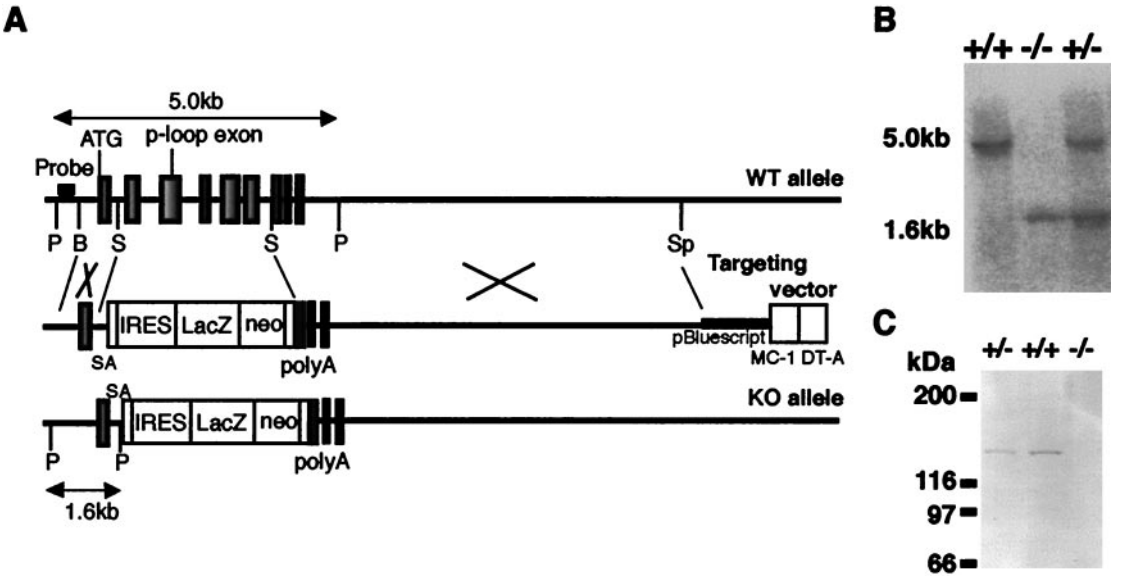

FIG. 2. Targeted disruption of the mouse *kif1C* gene. (A) Schematic drawing of the targeting strategy for *kif1C*. A 2.6-kb region (corresponding to aa 36 to 240) encoding the ATP binding motif P-loop was deleted and replaced with an SA-IRESβgeo cassette. A poly(A)-less diphtheria toxin A fragment (DT-A) was used as a negative selection marker. The probe used for screening the homologous recombination is also indicated. ATG, *kif1C* gene translation start site; P, *Pst*I; B, *Bam*HI; S, *Sma*I; Sp, *Spe*I; SA, splice acceptor sequence; WT, wild type; KO, knockout, (B) Southern blot analysis of genomic DNA isolated from mouse tail tissue. Genomic DNA was digested with *Pst*I and probed with a 240-bp fragment 5′ to the exon, yielding 5.0-kb restriction fragments from $kif1C^{+/+}$ alleles and 1.6-kb fragments from $kif1C^{-/-}$ alleles. (C) Immunoblot analysis of KIF1C expression in whole-brain homogenates (30 μg of protein) of respective genotypes with anti-KIF1C antibody. No bands were detected in the $kif1C^{-/-}$ samples.

that the homozygotes exhibit normal embryonic development. After birth, the homozygotes grew normally with no apparent changes in viability up to at least 18 months. $kif1C^{-/-}$ mice were fertile and indistinguishable in appearance from their $kif1C^{+/+}$ or $kif1C^{+/-}$ littermates. Immunoblotting of the whole-brain homogenate using the anti-KIF1C antibody confirmed the complete absence of KIF1C in the knockout brain (Fig. 2C).

We then assessed the expression pattern of KIF1C by LacZ staining. In accordance with the result of immunoblotting, strong staining was detected in the liver, heart, and kidneys. Weaker staining was also detected in the hippocampus and cerebellum (Fig. 3A to D).

However, histological analysis of the $kif1C^{-/-}$ mice showed no apparent histological abnormalities in those tissues (Fig. 3E to J).

KIF1C is not essential for the motor-dependent retrograde Golgi-to-ER transport. We studied the localization of KIF1C in hepatocytes by immunohistochemistry. The background staining in $kif1C^{-/-}$ tissue was significantly lower than the signal in $kif1C^{+/+}$ tissue. At higher magnification, an evident perinuclear signal was observed in each cell (Fig. 4A). Next, we studied the subcellular localization of KIF1C in primary fibroblasts by immunocytochemistry. The signal of KIF1C again showed a perinuclear pattern, which significantly overlapped that of the Golgi apparatus marker, CTR433 (12) (Fig. 4B), consistent with a previous report (5).

Figure 4B showed that the staining of KIF1C partially overlapped that of a Golgi marker, and a previous study had also suggested that KIF1C was involved in Golgi-to-ER transport (5). Therefore, we analyzed the dynamics of Golgi membranes in the KIF1C-deficient fibroblasts. First, we observed the steady-state Golgi distribution by immunocytochemistry using three specific antibodies against Golgi markers, GM-130, Vti1b, and p58 (Fig. 5). GM-130 is present in the Golgi matrix and is associated with the periphery of the *cis*-Golgi compartment (22). Vti1b is a putative mammalian SNARE protein that is required for vesicle fusion and docking at the Golgi apparatus (1). p58 is located specifically at the *cis*/medial site of the Golgi apparatus (3, 37). No significant difference in the Golgi shape was observed between $kif1C^{+/+}$ and $kif1C^{-/-}$ cells.

Next, to test the possibility that KIF1C is involved in the Golgi-to-ER transport, we examined the BFA-dependent breakdown of the Golgi apparatus by immunocytochemistry

of KIFs are shown in boldface type. The sequence of mKIF1A was truncated at aa 666, where an arrowhead shows the end of the conserved head domain among the KIF1 family. The AF6/cno domain is underlined. The FHA domain is shaded. The sequence against which the antibody was raised is doubly underlined. The alignment was performed using the ClustalW algorithm and manually modified. (B) Ubiquitous expression pattern of KIF1C protein in mouse tissues (40 μg of protein was loaded in each lane). (C) Subcellular fractionation of the MDCK cells monitored for KIF1C protein. KIF1C was most abundant in the high-speed membrane-pellet fraction (100,000 × *g* precipitate [ppt]). (D) Nucleotide-dependent binding activity of KIF1C to microtubules. The AMP-PNP pellet was resuspended in ATP-containing (0, 5, and 10 mM) buffer and centrifuged. The pellets (P) and the supernatants (S) were analyzed by immunoblotting. CE, crude extract. Note that KIF1C was released from microtubules depending on the concentration of ATP.

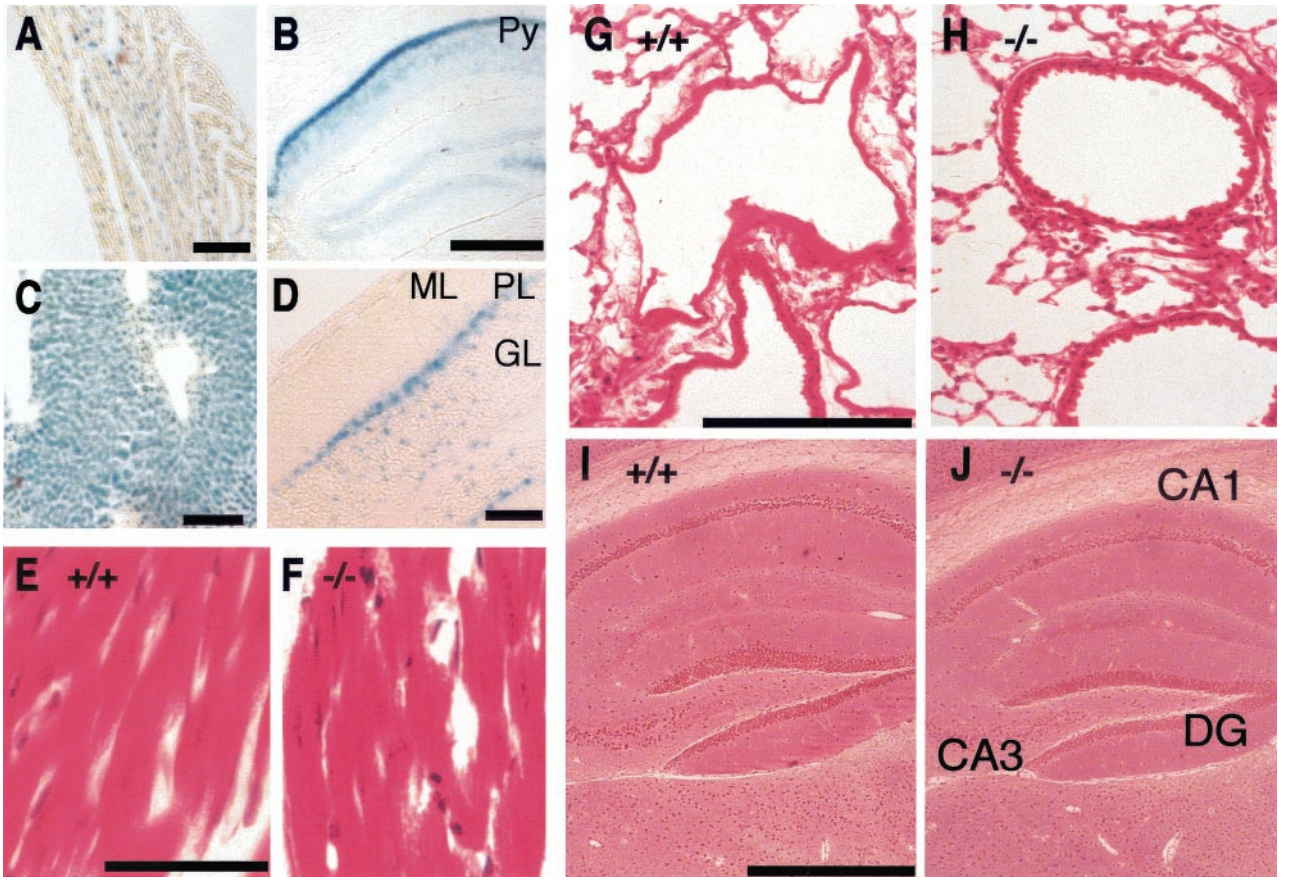

FIG. 3. Histological examination of the knockout mice. (A to D) Detection of *lacZ* gene expression from *kif1C*$^{+/-}$ mice. (A) Heart. Bar, 100 μm. (B) Coronal section of hippocampal region in brain. Py, pyramidal layer in hippocampus. Bar, 500 μm. (C) Liver. Bar, 100 μm. (D) Sagittal section of cerebellum. ML, molecular layer; PL, Purkinje cell layer; GL, granular layer. Bar, 100 μm. (E to J) Histological examination. (E, G, and I) *kif1C*$^{+/+}$ tissues; (F, H, and J) *kif1C*$^{-/-}$ tissues. There were no obvious structural changes in the tissues of the *kif1C*$^{-/-}$ mice. (E and F) Heart (hematoxylin and eosin stain). Bar, 10 μm. (G and H) Lung (hematoxylin and eosin stain). Bar, 200 μm. (I and J) Hippocampus (Bodian silver stain). Bar, 500 μm. DG, dentate gyrus; CA1, CA1 field; CA3, CA3 field.

using an anti-p58 antibody. After treatment of the cells with BFA, the staining pattern of p58 was redistributed from a juxtanuclear pattern to a cytoplasmic pattern in *kif1C*$^{-/-}$ cells as well as in *kif1C*$^{+/+}$ cells (Fig. 5B). Thus, BFA caused dispersion of the Golgi membrane in *kif1C*$^{-/-}$ cells.

These results, however, did not test the involvement of KIF1C in the microtubule-dependent active retrograde Golgi-to-ER transport; therefore, we performed a more detailed analysis of the Golgi-to-ER membrane dynamics by live-cell imaging. To analyze the dynamic properties of the Golgi membrane tubules, time-lapse recordings were performed of fibroblasts expressing an EYFP-galactosyltransferase fusion protein, which targeted the *trans*-medial region of the Golgi

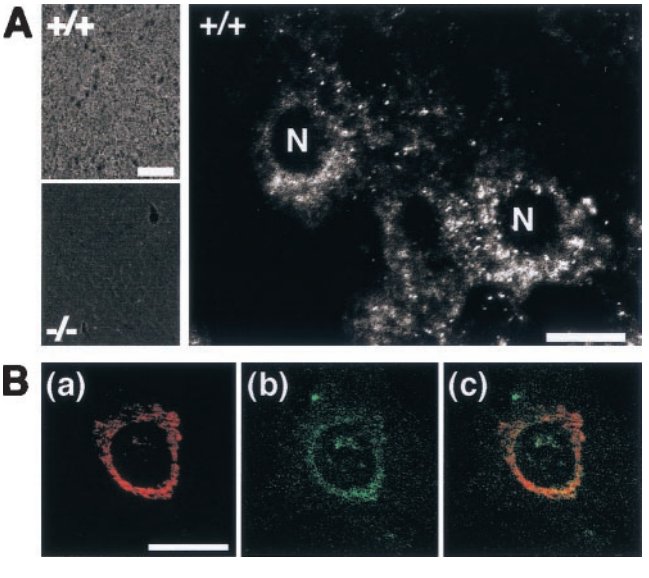

FIG. 4. Subcellular localization of KIF1C. (A) KIF1C signal in mouse liver. Note that the knockout tissue eliminated the signal (left, bottom). At higher magnification, the signal was localized in the perinuclear region of wild-type cells (right). N, nucleus. Bars, 200 μm (left) and 10 μm (right). (B) Intracellular localization of KIF1C. Fibroblasts were doubly stained with anti-Golgi CTR433 [red (a)] and anti-KIF1C [green (b)] antibodies. These two signals were mainly colocalized (C). Bar, 10 μm.

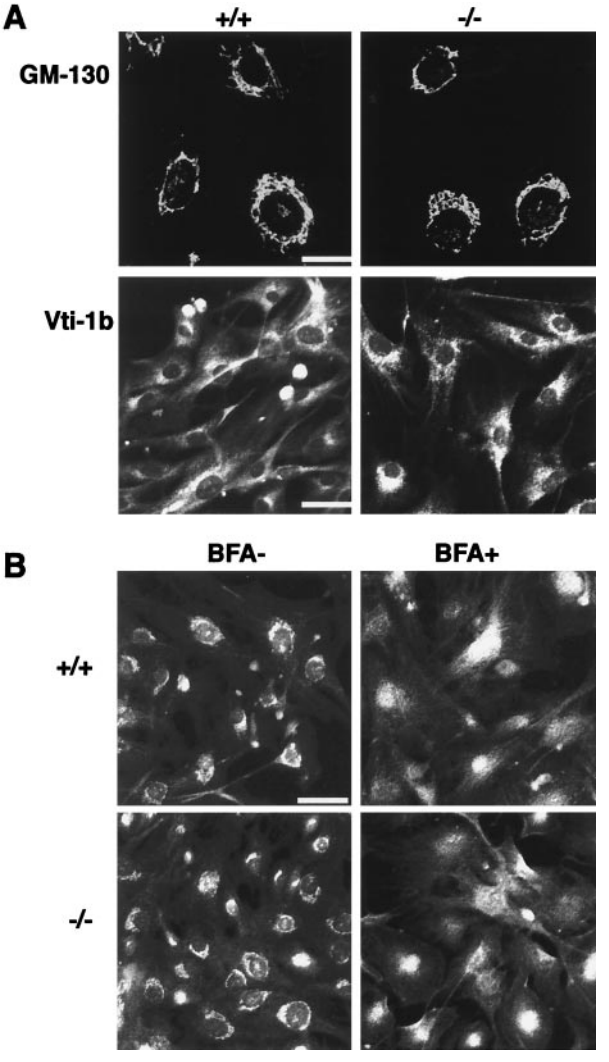

FIG. 5. Distribution and BFA-induced breakdown of the Golgi apparatus. (A) Comparison of the immunostaining pattern using antibodies against Golgi marker proteins. There were no significant differences in staining pattern between *kif1C*$^{+/+}$ and *kif1C*$^{-/-}$ cells. Bars, 25 μm (top) and 50 μm (bottom). (B) Disassembly of the Golgi apparatus facilitated by BFA. Cultured fibroblasts from *kif1C*$^{+/+}$ and *kif1C*$^{-/-}$ mice were immunostained for the Golgi marker protein p58 after the treatment of cells with BFA (5 μg/ml) for 10 min at 37°C. Golgi disassembly was observed in both types of cells. Bar, 50 μm.

apparatus. Thin tubular processes were equally observed to extend rapidly, break off, or detach from the rims of Golgi stacks after the treatment of *kif1C*$^{-/-}$ cells with BFA. The properties of the membrane tubule dynamics therefore appeared undisturbed compared to that of wild-type cells (Fig. 6). We measured the rate of change of the elongating or detaching tubules, where we found no significant difference between the genotypes. The mean velocities were 0.40 ± 0.15 μm/s in *kif1C*$^{+/+}$ cells and 0.35 ± 0.11 μm/s in *kif1C*$^{-/-}$ cells (n = 30). The number of tubules and the frequency of their extension per cell did not differ significantly between *kif1C*$^{+/+}$ and *kif1C*$^{-/-}$ cells. In conclusion, in contrast to the previous report, the motor-dependent Golgi-to-ER transport remained intact even in the absence of KIF1C.

DISCUSSION

This is the first report of the molecular cloning and gene targeting of the mouse *kif1C* gene. Amino acid sequence alignment confirmed that KIF1C belongs to the KIF1 subfamily because of its high similarity to KIF1Bα and KIF1A, especially in the motor head domain. Since the AF-6/cno and FHA domains are preserved, some cargo binding or regulating mechanisms are conserved among the KIF1 family members.

Next, we used a gene-targeting approach to reveal the func-

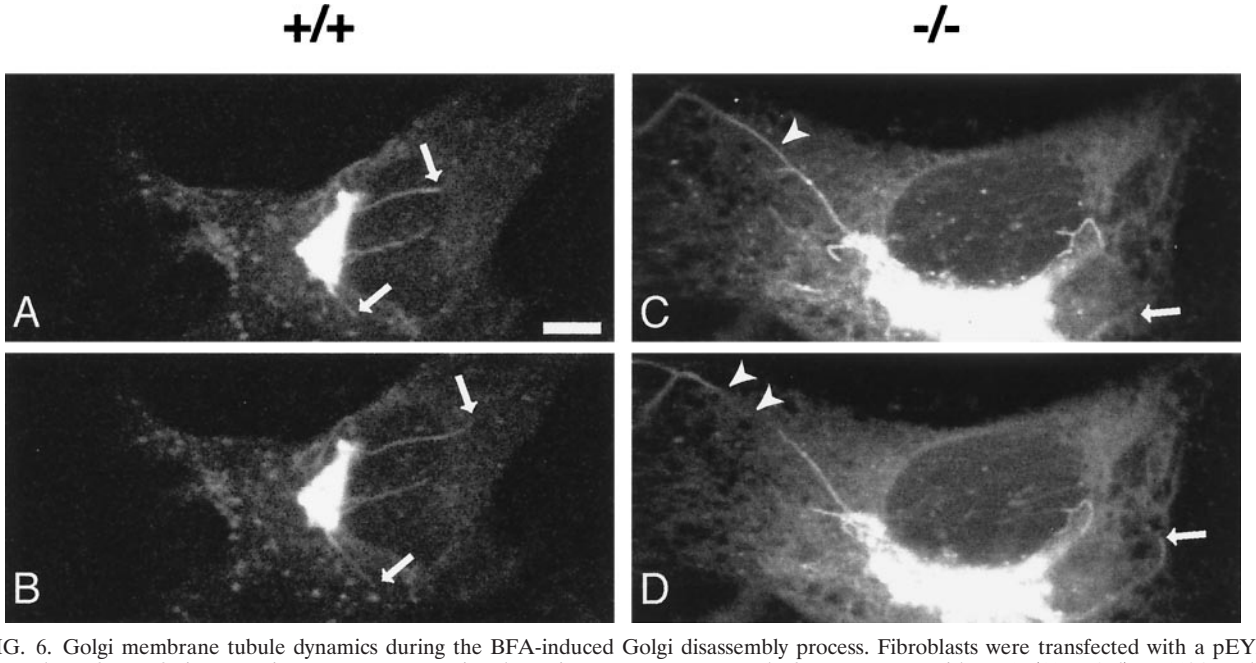

FIG. 6. Golgi membrane tubule dynamics during the BFA-induced Golgi disassembly process. Fibroblasts were transfected with a pEYFP-galactosyltransferase fusion protein gene construct. Time-lapse images were processed after treatment with BFA (10 μg/ml) at 30°C. Tubule formation from the Golgi apparatus was observed in each genotype. The intervals between the top (A and C) and bottom (B and D) frames were 20 s. Arrows indicate tips of growing tubules. Arrowheads indicate detaching tubules. Bar, 5 μm.

tion of KIF1C. Inspired by previous reports, we investigated the retrograde Golgi-to-ER transport facilitated by BFA in *kif1C*$^{-/-}$ cells. A motor-dependent retrograde Golgi-to-ER transport was represented by tubule formation (30). Figure 6 shows that the motor-dependent Golgi-to-ER transport is intact in *kif1C*$^{-/-}$ cells. This result is inconsistent with the result of a previous study involving a dominant negative form (5). It could be partially explained by the difference in cell types, but we suppose that it was derived from the difference in the experimental methods used. In gene targeting, we simply remove a motor so that the phenotype would not be apparent if some other motors compensate for the loss of that motor. In contrast, when we apply a dominant negative form of that motor, which makes its cargoes rigorously stick to the microtubules by stopping the ATPase cycle (23), the distribution of the cargo organelle will be altered irrespective of other compensatory motors. Retrograde Golgi-to-ER membrane transports have been reported to be driven by multiple motors such as the KIF3 complex (16), Rabkinesin 6 (6), and unknown H1 antigens other than KIF1C or conventional kinesin (29). Thus, it is possible that the Golgi dynamics of *kif1C*$^{-/-}$ cells was not changed, although a previously reported dominant negative form of KIF1C did block the Golgi-to-ER retrograde membrane transport. The present results indicate that KIF1C is not essential for the Golgi-to-ER transport. Although it does not exclude the possibility that KIF1C is still involved in that transport, our results indicate that KIF1C by itself is not essential for this process, contrary to the previous expectations. Although the Golgi-to-ER transport was intact in *kif1C*$^{-/-}$ cells, the result that the staining of KIF1C partially colocalized with that of the Golgi marker protein (Fig. 4B) implies that KIF1C may be involved in transport around the Golgi apparatus other than the Golgi-to-ER transport. Future double-knockout studies with other KIF knockout mice would be helpful to clarify the contribution of KIF1C to intracellular transport including Golgi-to-ER transport.

ACKNOWLEDGMENTS

We are grateful to A. Harada, Y. Kanai, S. Takeda, Y. Xu, and other members of the Hirokawa laboratory for suggestions and discussions. We also thank H. Sato, H. Fukuda, M. Sugaya, and N. Onouchi for technical and secretarial assistance.

This work was supported by a Center of Excellence (COE) grant-in-aid to N.H. from the Ministry of Education, Science, Sports, Culture and Technology of Japan.

REFERENCES

1. **Advani, R. J., H. R. Bae, J. B. Bock, D. S. Chao, Y. C. Doung, R. Prekeris, J. S. Yoo, and R. H. Scheller.** 1998. Seven novel mammalian SNARE proteins localize to distinct membrane compartments. J. Biol. Chem. **273:**10317–10324.
2. **Aizawa, H., Y. Sekine, R. Takemura, Z. Zhang, M. Nangaku, and N. Hirokawa.** 1992. Kinesin family in murine central nervous system. J. Cell Biol. **119:**1287–1296.
3. **Bloom, G. S., and T. A. Brashear.** 1989. A novel 58-kDa protein associates with the Golgi apparatus and microtubules. J. Biol. Chem. **264:**16083–16092.
4. **Bodian, P.** 1936. A new method for staining nerve fibers and nerve ending in mounted paraffin sections. Anat. Rec. **65:**89–96.
5. **Dorner, C., T. Ciossek, S. Muller, P. H. Moller, A. Ullrich, and R. Lammers.** 1998. Characterization of KIF1C, a new kinesin-like protein involved in vesicle transport from the Golgi apparatus to the endoplasmic reticulum. J. Biol. Chem. **273:**20267–20275.
6. **Echard, A., F. Jollivet, O. Martinez, J. J. Lacapere, A. Rousselet, I. Janoueix-Lerosey, and B. Goud.** 1998. Interaction of a Golgi-associated kinesin-like protein with Rab6. Science **279:**580–585.
7. **Freshney, I. R.** 1994. Culture of animal cells. Wiley-Liss, New York, N.Y.
8. **Harada, A., K. Oguchi, S. Okabe, J. Kuno, S. Terada, T. Ohshima, R. Sato-Yoshitake, Y. Takei, T. Noda, and N. Hirokawa.** 1994. Altered microtubule organization in small-calibre axons of mice lacking tau protein. Nature **369:**488–491.
9. **Hayflick, L.** 1965. The limited in vitro lifetime of human diploid cell strains. Exp. Cell Res. **37:**614–636.
10. **Hirokawa, N.** 1998. Kinesin and dynein superfamily proteins and the mechanism of organelle transport. Science **279:**519–526.
11. **Hogan, B.** 1994. Manipulating the mouse embryo: a laboratory manual, 2nd ed. Cold Spring Harbor Laboratory Press, Plainview, N.Y.
12. **Jasmin, B. J., J. Cartaud, M. Bornens, and J. P. Changeux.** 1989. Golgi apparatus in chick skeletal muscle: changes in its distribution during end plate development and after denervation. Proc. Natl. Acad. Sci. USA **86:**7218–7222.
13. **Joyner, A. L.** 1993. Gene targeting: a practical approach. Oxford University Press, Oxford, United Kingdom.
14. **Kanai, Y., Y. Okada, Y. Tanaka, A. Harada, S. Terada, and N. Hirokawa.** 2000. KIF5C, a novel neuronal kinesin enriched in motor neurons. J. Neurosci. **20:**6374–6384.
15. **Klausner, R. D., J. G. Donaldson, and J. Lippincott-Schwartz.** 1992. Brefeldin A: insights into the control of membrane traffic and organelle structure. J. Cell Biol. **116:**1071–1080.
16. **Le Bot, N., C. Antony, J. White, E. Karsenti, and I. Vernos.** 1998. Role of Xklp3, a subunit of the *Xenopus* kinesin II heterotrimeric complex, in membrane transport between the endoplasmic reticulum and the Golgi apparatus. J. Cell Biol. **143:**1559–1573.
17. **Lippincott-Schwartz, J., J. G. Donaldson, A. Schweizer, E. G. Berger, H. P. Hauri, L. C. Yuan, and R. D. Klausner.** 1990. Microtubule-dependent retrograde transport of proteins into the ER in the presence of brefeldin A suggests an ER recycling pathway. Cell **60:**821–836.
18. **Lippincott-Schwartz, J., L. Yuan, C. Tipper, M. Amherdt, L. Orci, and R. D. Klausner.** 1991. Brefeldin A's effects on endosomes, lysosomes, and the TGN suggest a general mechanism for regulating organelle structure and membrane traffic. Cell **67:**601–616.
19. **Miki, H., M. Setou, K. Kaneshiro, and N. Hirokawa.** 2001. All kinesin superfamily protein, KIF, genes in mouse and human. Proc. Natl. Acad. Sci. USA **98:**7004–7011.
20. **Nakagawa, T., M. Setou, D. Seog, K. Ogasawara, N. Dohmae, K. Takio, and N. Hirokawa.** 2000. A novel motor, KIF13A, transports mannose-6-phosphate receptor to plasma membrane through direct interaction with AP-1 complex. Cell **103:**569–581.
21. **Nakagawa, T., Y. Tanaka, E. Matsuoka, S. Kondo, Y. Okada, Y. Noda, Y. Kanai, and N. Hirokawa.** 1997. Identification and classification of 16 new kinesin superfamily (KIF) proteins in mouse genome. Proc. Natl. Acad. Sci. USA **94:**9654–9659.
22. **Nakamura, N., M. Lowe, T. P. Levine, C. Rabouille, and G. Warren.** 1997. The vesicle docking protein p115 binds GM130, a cis-Golgi matrix protein, in a mitotically regulated manner. Cell **89:**445–455.
23. **Nakata, T., and N. Hirokawa.** 1995. Point mutation of adenosine triphosphate-binding motif generated rigor kinesin that selectively blocks anterograde lysosome membrane transport. J. Cell Biol. **131:**1039–1053.
24. **Nakata, T., S. Terada, and N. Hirokawa.** 1998. Visualization of the dynamics of synaptic vesicle and plasma membrane proteins in living axons. J. Cell Biol. **140:**659–674.
25. **Nangaku, M., R. Sato-Yoshitake, Y. Okada, Y. Noda, R. Takemura, H. Yamazaki, and N. Hirokawa.** 1994. KIF1B, a novel microtubule plus end-directed monomeric motor protein for transport of mitochondria. Cell **79:**1209–1220.
26. **Nonaka, S., Y. Tanaka, Y. Okada, S. Takeda, A. Harada, Y. Kanai, M. Kido, and N. Hirokawa.** 1998. Randomization of left-right asymmetry due to loss of nodal cilia generating leftward flow of extraembryonic fluid in mice lacking KIF3B motor protein. Cell **95:**829–837.
27. **Okada, Y., H. Yamazaki, Y. Sekine-Aizawa, and N. Hirokawa.** 1995. The neuron-specific kinesin superfamily protein KIF1A is a unique monomeric motor for anterograde axonal transport of synaptic vesicle precursors. Cell **81:**769–780.
28. **Ponting, C. P.** 1995. AF-6/cno: neither a kinesin nor a myosin, but a bit of both. Trends Biochem. Sci. **20:**265–266.
29. **Robertson, A. M., and V. J. Allan.** 2000. Brefeldin A-dependent membrane tubule formation reconstituted in vitro is driven by a cell cycle-regulated microtubule motor. Mol. Biol. Cell **11:**941–955.
30. **Sciaky, N., J. Presley, C. Smith, K. J. Zaal, N. Cole, J. E. Moreira, M. Terasaki, E. Siggia, and J. Lippincott-Schwartz.** 1997. Golgi tubule traffic and the effects of brefeldin A visualized in living cells. J. Cell Biol. **139:**1137–1155.
31. **Setou, M., T. Nakagawa, D. H. Seog, and N. Hirokawa.** 2000. Kinesin superfamily motor protein KIF17 and mLin-10 in NMDA receptor-containing vesicle transport. Science **288:**1796–1802.
32. **Takeda, S., H. Yamazaki, D. H. Seog, Y. Kanai, S. Terada, and N. Hirokawa.** 2000. Kinesin superfamily protein 3 (KIF3) motor transports fodrin-associating vesicles important for neurite building. J. Cell Biol. **148:**1255–1265.
33. **Takeda, S., Y. Yonekawa, Y. Tanaka, Y. Okada, S. Nonaka, and N. Hiro-**

kawa. 1999. Left-right asymmetry and kinesin superfamily protein KIF3A: new insights in determination of laterality and mesoderm induction by *kif3A*$^{-/-}$ mice analysis. J. Cell Biol. **145:**825–836.
34. **Tanaka, Y., Y. Kanai, Y. Okada, S. Nonaka, S. Takeda, A. Harada, and N. Hirokawa.** 1998. Targeted disruption of mouse conventional kinesin heavy chain, *kif5B*, results in abnormal perinuclear clustering of mitochondria. Cell **93:**1147–1158.
35. **Wagner, M. C., K. K. Pfister, S. T. Brady, and G. S. Bloom.** 1991. Purification of kinesin from bovine brain and assay of microtubule-stimulated ATPase activity. Methods Enzymol. **196:**157–175.
36. **Watakabe, A., K. Tanaka, and Y. Shimura.** 1993. The role of exon sequences in splice site selection. Genes Dev. **7:**407–418.
37. **Wehland, J., and M. C. Willingham.** 1983. A rat monoclonal antibody reacting specifically with the tyrosylated form of alpha-tubulin. II. Effects on cell movement, organization of microtubules, and intermediate filaments, and arrangement of Golgi elements. J. Cell Biol. **97:**1476–1490.
38. **Westerholm-Parvinen, A., I. Vernos, and L. Serrano.** 2000. Kinesin subfamily UNC104 contains a FHA domain: boundaries and physicochemical characterization. FEBS Lett. **486:**285–290.
39. **Yagi, T., S. Nada, N. Watanabe, H. Tamemoto, N. Kohmura, Y. Ikawa, and S. Aizawa.** 1993. A novel negative selection for homologous recombinants using diphtheria toxin A fragment gene. Anal. Biochem. **214:**77–86.
40. **Yonekawa, Y., A. Harada, Y. Okada, T. Funakoshi, Y. Kanai, Y. Takei, S. Terada, T. Noda, and N. Hirokawa.** 1998. Defect in synaptic vesicle precursor transport and neuronal cell death in KIF1A motor protein-deficient mice. J. Cell Biol. **141:**431–441.
41. **Zhao, C., J. Takita, Y. Tanaka, M. Setou, T. Nakagawa, S. Takeda, H. W. Yang, S. Terada, T. Nakata, Y. Takei, M. Saito, S. Tsuji, Y. Hayashi, and N. Hirokawa.** 2001. Charcot-Marie-Tooth disease type 2A caused by mutation in a microtubule motor KIF1Bβ. Cell **105:**587–597.